OXFORD

SOT | Society of Toxicology
www.toxsci.oxfordjournals.org

TOXICOLOGICAL SCIENCES, 159(1), 2017, 170–178

doi: 10.1093/toxsci/kfx126
Advance Access Publication Date: June 19, 2017
Research Article

Lateralized Basal Ganglia Vulnerability to Pesticide Exposure in Asymptomatic Agricultural Workers

Mechelle M. Lewis,[*,†] Nicholas W. Sterling,[*] Guangwei Du,[*] Eun-Young Lee,[*] Grace Shyu,[*] Michael Goldenberg,[*] Thomas Allen,[‡] Christy Stetter,[‡] Lan Kong,[‡] Shedra Amy Snipes,[§] Byron C. Jones,[¶] Honglei Chen,[‖] Richard B. Mailman,[*,†] and Xuemei Huang[*,†,‡,1]

[*]Department of Neurology; [†]Department of Pharmacology; [‡]Department of Radiology, and Department of Public Health Sciences, Pennsylvania State University-Milton S. Hershey Medical Center, Hershey, Pennsylvania 17033; [§]Department of Biobehavioral Health, Pennsylvania State University University Park, Pennsylvania 16802; [¶]Department of Genetics, Genomics and Informatics, University of Tennessee Health Science Center, Memphis, Tennessee 38163; and [‖]Department of Epidemiology and Biostatistics, Michigan State University, East Lansing, Michigan 48824

[1]To whom correspondence should be addressed at Department of Neurology, Pennsylvania State University, H037, 500 University Drive, Hershey, PA 17033-0850. Fax: (717) 531-0266. E-mail: xuemei@psu.edu.

ABSTRACT

Pesticide exposure is linked to Parkinson's disease, a neurodegenerative disorder marked by dopamine cell loss in the substantia nigra of the basal ganglia (BG) that often presents asymmetrically. We previously reported that pesticide-exposed agricultural workers (AW) have nigral diffusion tensor imaging (DTI) changes. The current study sought to confirm this finding, and explore its hemisphere and regional specificity within BG structures using an independent sample population. Pesticide exposure history, standard neurological exam, high-resolution magnetic resonance imaging (T1/T2-weighted and DTI), and [^{123}I]ioflupane SPECT images (to quantify striatal dopamine transporters) were obtained from 20 AW with chronic pesticide exposure and 11 controls. Based on median cumulative days of pesticide exposure, AW were subdivided into high (AW_{Hi}, $n = 10$) and low (AW_{Lo}, $n = 10$) exposure groups. BG (nigra, putamen, caudate, and globus pallidus [GP]) fractional anisotropy (FA), mean diffusivity (MD), and striatal [^{123}I]ioflupane binding in each hemisphere were quantified, and compared across exposure groups using analysis of variance. Left, but not right, nigral and GP FA were significantly lower in AW compared with controls (p's $< .029$). None of the striatal (putamen and caudate) DTI or [^{123}I]ioflupane binding measurements differed between AW and controls. Subgroup analyses indicated that significant left nigral and GP DTI changes were present only in the AW_{Hi} ($p \leq .037$) but not the AW_{Lo} subgroup. AW, especially those with higher pesticide exposure history, demonstrate lateralized microstructural changes in the nigra and GP, whereas striatal areas appear relatively unaffected. Future studies should elucidate how environmental toxicants cause differential lateralized- and regionally specific brain vulnerability.

Key words: substantia nigra; striatum; globus pallidus; MRI; DAT scan; pesticide exposure.

Parkinson's disease (PD) is marked primarily by loss of dopamine neurons in the substantia nigra (SN) of the basal ganglia (BG) and striatal dopamine deficiency (Dickson *et al.*, 2009; Fearnley and Lees, 1991). The fact that identical twins frequently are discordant for PD suggests that environmental factors may be associated with the etiology of sporadic PD through mechanisms such as oxidative stress, neuroinflammation, and/or cytotoxicity (Tanner *et al.*, 1999; Wirdefeldt *et al.*,

2004). Recent epidemiologic data support the hypothesis that pesticide exposure is associated with increased risk of PD (McCormack *et al.* 2002; Pezzoli and Cereda, 2013; Tanner *et al.*, 2011). In addition, a number of pesticides (eg, paraquat, rotenone, maneb) can cause direct dopaminergic toxicity in animal models (Desplats *et al.*, 2012; Uversky, 2004).

The onset of PD motor symptoms is typically asymmetric (Riederer and Sian-Hulsmann, 2012) and more often present on the right side of the body (Uitti *et al.*, 2005). Several studies have sought to identify a cause for this laterality. For example, asymmetrical changes in dopamine transporter levels have been reported in the striatum of PD patients (Siebyl *et al.*, 1995), but the exact causes and mechanisms of the lateralized vulnerability to PD are unknown.

Recently, magnetic resonance imaging (MRI) has been used extensively to study PD-related pathological changes in human subjects (Chan *et al.*, 2007; Du *et al.*, 2012; Martin *et al.*, 2008; Vaillancourt *et al.*, 2009). In particular, diffusion tensor imaging (DTI), by measuring microstructural organization or integrity, has shown promise as a tool for assessing PD-related nigral changes probably due to dopamine cell loss (Chan *et al.*, 2007; Du *et al.*, 2011; Peran *et al.*, 2010). In the MPTP PD mouse model, DTI changes are correlated with dopamine neuron loss in the SN (Boska *et al.*, 2007). Furthermore, several human studies have demonstrated reduced FA values in the SN of early PD patients, consistent with the notion that DTI changes may be able to detect nigral microstructural changes and track their progression *in vivo* (Du *et al.*, 2012; Ofori *et al.*, 2015; Vaillancourt *et al.*, 2009).

We recently demonstrated decreased diffusion measures in asymptomatic agricultural workers (AW) exposed to pesticides (Du *et al.*, 2014), providing the first direct evidence that chronic pesticide exposure may lead to nigral microstructural changes in humans that are qualitatively similar to PD. In this study, we first sought to confirm this finding, and then investigate whether changes occurred in a lateralized- and regionally specific manner within BG structures using MRI DTI (to reflect microstructural integrity). We hypothesized that: (1) other BG structures also may be susceptible to pesticide-related neurotoxicity; and (2) left side BG structures may be more vulnerable to pesticides because PD often presents with right side symptoms (Uitti *et al.*, 2005). Second, we examined nigrostriatal integrity via [^{123}I]ioflupane SPECT (single photon emission computed tomography) imaging (to visualize striatal dopamine transporters). Striatal dopaminergic terminal deficits are an essential feature of PD. We hypothesized that striatal dopaminergic transporter binding would be lower in AW with a history of pesticide exposure since our previous study (Du *et al.*, 2014) showed that AW had similar, but less severe, nigral microstructural changes (Du *et al.*, 2012; Ofori *et al.*, 2015; Vaillancourt *et al.*, 2009). Third, we investigated the relationships between BG imaging measurements and pesticide exposure. We hypothesized that: (1) subjects with longer durations of pesticide exposure will be more likely to have BG imaging changes; and (2) the BG imaging changes will be correlated with duration of pesticide exposure. Lastly, we explored the relationship between significant MRI DTI changes and dopamine transporter density.

MATERIALS AND METHODS

Subjects

A total of 20 AW and 11 controls were recruited from regional AW meetings in central Pennsylvania, USA, and from the community around the Penn State Hershey Medical Center (PSHMC). Those contacting us and expressing an interest in the study were screened for inclusion/exclusion criteria that included age 45-75 years, able/willing to provide consent, no significant memory impairment (Mini Mental Status Exam (MMSE) $>$ 24), normal kidney or liver function, no significant medical and or neurological deficits, and no claustrophobia or other condition precluding an MRI. AW were defined as subjects who had applied pesticides at any point in their lifetime and controls as those who did not have any history of pesticide exposure. Seven subjects (1 control and 6 AW) participated in a previous study focused on pesticide exposure effects on MRI measures in the SN (Du *et al.*, 2014). Subjects were all male and answered negatively for past diagnosis of neurological disorders. As part of the screening visit, detailed demographic information was obtained from all subjects. Since all subjects in the overall cohort were male, matching by gender was not an issue for the current study. Written informed consent was obtained from all subjects in accordance with the Declaration of Helsinki, and approved by the PHMC Internal Review Board/Human Subjects Protection Office.

Clinical Information

Height and weight were measured to calculate body mass index (BMI) for each subject. Handedness was determined by the dominant hand used during writing and eating, and all subjects were right-handed except for 1 control subject. A fasting blood sample was collected the morning of the study visit and assayed at the PSHMC clinical lab to rule out major medical issues (such as anemia, renal or liver dysfunctions). All subjects were examined and ascertained to be free of any obvious neurological and movement deficits using the UPDRS motor scores (UPDRS-III) with a threshold score of $<$15 indicating lack of parkinsonian motor signs as defined by a previous study (Lee *et al.*, 2015). The UPDRS-III exams were performed by trained raters according to the Movement Disorder Society training modules. Subjects also completed sections I (a nonmotor-related functional questionnaire) and II (a motor-related functional questionnaire) of the UPDRS.

Exposure Assessment

Pesticide exposure was evaluated using a validated and detailed questionnaire from the Agriculture Health Study (AHS). The AHS is a large prospective study of the National Institute of Environmental Health Sciences that examines health effects among AW who have been exposed to pesticides (http://www.niehs.nih.gov). Using the AHS questionnaire, we evaluated frequency (ie, average annual number of days used) and duration (ie, number of exposed years) of pesticide exposures, including types of pesticide handled (ie, mixing, loading, and/or application), personal protective equipment use, and personal hygiene practices. Pesticides assessed were selected because of their frequency and overall use in the agricultural settings of central Pennsylvania, or because of human or animal data suggesting their possible adverse health effects. The pesticides to which subjects were exposed are listed in Supplementary Table 1.

Pesticide exposures in AW and control subjects were calculated based on the number of days of exposure. AW then were dichotomized into 2 groups based on the median: low exposure AW (AW_{Lo}) and high exposure AW (AW_{Hi}). The dichotomized exposure variable was the main exposure metric for all subjects.

Imaging Data Acquisition

Brain MRI data acquisition. All subjects were scanned with a 3.0 Tesla MRI system (Trio, Siemens Magnetom, Erlangen, Germany, 8-channel phased array head coil) with high-

resolution T1-, T2-weighted, and DTI sequences. A 3D MPRAGE with TR = 1540 ms, TE = 2.3 ms, isotropic 1-mm voxels was utilized to acquire T1-weighted images. A fast-spin-echo sequence was used to obtain T2-weighted images with TR/TE = 2500/316, FOV = 256 × 256 mm, matrix = 256 × 256, slice thickness = 1 mm (with no gap), and slice number = 176. For DTI, acquisition parameters were as follows: TR/TE = 8300/82 ms, b value = 1000 s/mm^2, diffusion gradient directions = 42 and 7 b = 0 scans, FOV = 256 × 256 mm, matrix = 128 × 128, slice thickness = 2 mm (with no gap), and slice number = 65.

Dopamine transporter data acquisition. [^{123}I]Ioflupane (DaTscan, GE Healthcare, Ltd, Marlborough, Massachusetts) was used to image dopamine transporters. Subjects ingested Lugol's solution diluted in water (equivalent to 100 mg of iodide) to protect the thyroid gland. An IV line was placed by an experienced nurse and 1 h after ingestion of the iodide solution, subjects were injected with 4 mCi of [^{123}I]ioflupane. Images of the brain were acquired 4 h later using a SPECT camera (Siemens, Symbia Evo) with the recommended imaging parameters (Kupsch *et al.*, 2012). The reconstructed images then were transferred to a secure research picture archiving and communication system for further analysis.

Data Analysis

Segmentation of BG structures on MRI. The SN was defined manually on T2-weighted images using ITK-SNAP (Yushkevich *et al.*, 2006) by an investigator blinded to subject identification. This region of interest was defined as a hypointense band between the red nucleus (RN) and cerebral peduncle (CP) in axial sections (Du *et al.*, 2011; Massey and Yousry, 2010; Vaillancourt *et al.*, 2012), as illustrated in Figure 1A. The most superior extent of the SN segmentation was defined at 1 slice inferior to the axial section of the RN showing the largest radius. A total of 4–6 slices (from the rostral to caudal part of the SNpc) were used as the SN region of interest (ROI) (Yushkevich *et al.*, 2006). The right and left SN were analyzed separately. Another set of SN ROIs also was obtained by a second rater (MG) using the same segmentation protocol, thus providing an estimate of the inter-rater reliability using intra-class correlation coefficients. Putamen (Put), caudate, and globus pallidus (GP) ROIs were defined on high-resolution T1-weighted images using multi-atlas automatic segmentation software (AutoSeg) for each subject (Gouttard *et al.*, 2007; Figure 1B).

Estimation of DTI measures. DTI image quality control and tensor reconstruction was performed using DTIPrep (Neuro Image Research and Analysis Laboratory, University of North Carolina, Chapel Hill, North Carolina, USA) that first checks DWI images for appropriate quality by calculating the inter-slice and inter-image intra-class correlation, and then corrects for the distortions induced by eddy currents and head motion (Liu *et al.*, 2010). Diffusion tensor images then were estimated via weighted least squares (Salvador *et al.*, 2005). DTI is thought to reflect the diffusion of water molecules in tissues and thus is an indicator of the structural organization in a region. Two DTI values (fractional anisotropy [FA] and mean diffusivity [MD]) were calculated out of 3 diffusivity eigenvalues (λ1, λ2, λ3; Le Bihan *et al.*, 2001). FA is a weighted average of pairwise differences of the 3 eigenvalues and may reflect the degree of diffusion anisotropy.

$$FA = \sqrt{\frac{1\sqrt{(\lambda_1-\lambda_2)^2+(\lambda_2-\lambda_3)^2+(\lambda_3-\lambda_1)^2}}{2\sqrt{\lambda_1^2+\lambda_2^2+\lambda_3^2}}}$$

MD is an average of the 3 eigenvalues and provides information regarding the magnitude of the diffusion (Du *et al.*, 2014; Le Bihan *et al.*, 2001; Lee *et al.*, 2016).

The segmented bilateral ROIs were mapped to FA maps by co-registering the T2-weighted images to the B0 images of DTI data using an affine registration pipeline implemented in 3D Slicer (www.slicer.org) (Rueckert *et al.*, 1999). Mean FA and MD values then were obtained for further analysis.

Quantification of striatal DAT binding. To obtain striatal regions of interest, a common atlas was first generated from all acquired [^{123}I]ioflupane (dopamine transporter [DAT]-binding density) images. The striatum was delineated manually on this common atlas, and divided into the anterior and posterior divisions to separate the caudate from the Put (Seibyl *et al.*, 1995). Subject images first were aligned to a common atlas via linear affine registration (Avants *et al.*, 2011). Mean signal intensity values were extracted from the delineated striatal ROIs on each subject

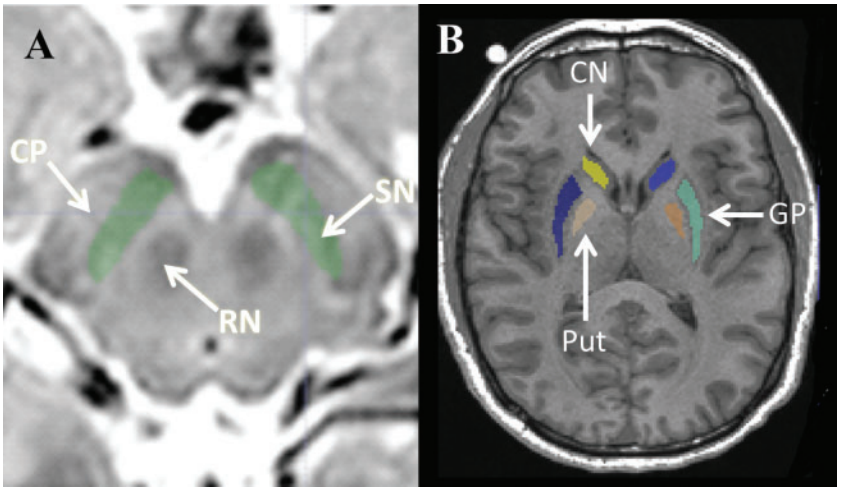

Figure 1. Schematic of the segmentation of BG structures. A, Illustration of ROI definition of the SN. The arrows indicate the SN, RN, and CP. B, Illustration of the ROI definition of the caudate (CN), Put, and GP. Regions are indicated by arrows.

Table 1. Demographic and Clinical Characteristics of Study Subjects

	Controls	AWs			Group comparisons			
		AW	AW_{Lo}	AW_{Hi}	Controls vs. AW	Controls vs. AW_{Lo}	Controls vs. AW_{Hi}	AW_{Lo} vs. AW_{Hi}
Number (n)	11	20	10	10				
Age	59.1 ± 10.1	59.4 ± 7.4	60.6 ± 8.7	58.2 ± 5.9	0.923	0.688	0.812	0.534
BMI	27.2 ± 2.5	29.4 ± 3.8	29.2 ± 3.4	29.6 ± 4.2	0.102	0.206	0.130	0.798
Days of exposure[a]	0	638 (105–6825)	245 (105–525)	1750 (750–6825)				
MMSE	29.8 ± 0.4	28.7 ± 1.3	28.2 ± 1.3	29.1 ± 1.0	0.783	0.754	0.876	0.876
UPSIT	31.5 ± 4.3	32.0 ± 5.0	29.7 ± 5.7	34.3 ± 3.0	0.790	0.376	0.173	0.030
UPDRS								
UPDRS-I	0.5 ± 0.7	0.9 ± 1.3	0.6 ± 0.8	1.1 ± 1.7	0.480	0.913	0.273	0.333
UPDRS-II	2.1 ± 2.5	2.8 ± 3.0	2.3 ± 3.0	3.3 ± 3.1	0.508	0.867	0.337	0.437
UPDRS-III	2.5 ± 2.3	4.8 ± 3.6	5.2 ± 3.5	4.4 ± 3.9	0.062	0.064	0.182	0.587

Data represent the mean ± SD unless otherwise indicated. Each measure was compared using either *t* tests (controls vs. AWs) or ANOVA (for the comparisons among controls, AW_{Lo}, and AW_{Hi}). BMI, Body mass index; MoCA, Montreal Cognitive Assessment; UPDRS, Unified Parkinson's Disease Rating Scale; UPSIT, University of Pittsburgh Smell Identification Test.

[a]Days of exposure for AWs and their subgroups are reported as median and range. The groups were not compared since controls had 0 days of exposure and thus statistics were not appropriate.

image. Striatal binding was normalized for each image by subtracting the mean signal intensity region of an occipital ROI from the striatal intensity (Seibyl *et al.*, 1995). All striatal measurements are reported according to hemisphere location, with each region separated into the anterior (caudate) and posterior (Put) areas. Hereafter, we refer to the results as DAT binding (ie, relative DAT density).

Inter-Rater Validation of DTI Measurements

There was moderate agreement between the 2 raters regarding the segmentation and resulting extraction of DTI measures in the SN. The inter-rater agreement using concordance correlation coefficients (CCCs) were 0.74 for left FA and 0.69 for right FA. The CCCs were 0.64 for left MD and 0.67 for right MD. The results presented in this article are based on the data from one rater, although an independent analysis of the ROIs from the second rater yielded similar results (data not shown).

Statistical Analysis

Demographic and clinical measures were compared between controls and AW as a whole using t-tests, whereas those among controls, low exposure (AW_{Lo}), and high exposure (AW_{Hi}) AW were conducted using 1-way analysis of variance (ANOVA). Basal ganglia DTI (FA and MD) and DAT-binding (anterior and posterior striatal regions) measures were compared between each hemisphere by paired *t* tests within controls, AW, or AW subgroups. Then, BG DTI (FA and MD) and DAT-binding (anterior and posterior striatal regions) measures were compared between controls and the agricultural group or subgroups by 1-way analysis of covariance (ANCOVA) with adjustment for age. We explored the associations between BG DTI measures and days of pesticide exposure using Spearman partial correlations while adjusting for age. Last, we explored the relationship between significant DTI measures and striatal DAT binding measurements adjusting for age. Due to the explorative nature, we did not control for multiple comparisons. Significance was defined as $p < .05$ and marginal significance as $p \geq .05$ and $<.10$. All statistical analyses were performed using SAS 9.3 with 2-sided alphas (SAS Institute Inc., Cary, North Carolina, USA).

RESULTS

Demographic Data

There were no differences in age, BMI, University of Pittsburgh Smell Identification Test, MMSE, UPDRS-I, or UPDRS-II scores between controls and AW (Table 1). In contrast, AW tended to have higher UPDRS-III scores than controls ($p = .062$; Table 1).

Exposure Assessment

Intrinsic to our study design, AW had more days of exposure compared with controls. The range of exposure duration, however, was extremely wide and a few subjects had extremely long exposure durations (see Supplementary Figures). The median cumulative days of pesticide exposure for all AW was 638 days (range = 105–6825). The median number of days for the AW_{Lo} subgroup was 245 days (range = 105-525), whereas that for the AW_{Hi} subgroup was 1750 days (range = 750–6825 days).

Diffusion Imaging Measures

Lateralized differences in DTI measurements. Within controls, the left FA values in the Put ($p = .021$) and GP ($p = 0.039$) were significantly higher than those on the right, and a similar but nonstatistically significant difference was observed for the SN ($p = .058$). The left MD in the SN ($p = .030$), Put ($p = .0004$), and GP ($p < .0001$) were significantly lower than on the right. There were no statistically significant hemisphere differences in the caudate.

Within AW overall, the left FA value was significantly higher in the Put ($p = .002$) and GP ($p = .001$) compared with the right side (a finding similar to that observed in controls), but there were no differences in the SN or caudate ($p \geq .19$). Similar findings for MD values were seen in the overall AW group, with lower Put ($p < .0001$) and GP ($p < .0001$) MD measures in the left compared with the right but no difference in the SN or caudate.

Within the AW subgroups, left FA values in the Put ($p = .002$) and GP ($p = .002$) were significantly higher in AW_{Lo} but not AW_{Hi} ($p \geq .14$) subjects. The left MD values were significantly lower in both AW_{Lo} ($p \leq .0003$) and AW_{Hi} ($p \leq .018$) subjects than those on the right, with a trend for the SN in AW_{Lo} subjects ($p = .062$).

Differences in DTI measurements between controls and AWs. When compared with controls, AW had lower left, but not right, SN and GP FA values after adjusting for age ($p \leq .029$, Table 2). There were no significant differences in bilateral striatal (caudate or Put) DTI measurements (FA or MD) between AW and controls.

The subgroup comparisons revealed that AW_{Hi}, but not AW_{Lo}, subjects showed significantly lower left nigral and GP ($p \leq .037$) FA values compared with controls. Trend MD differences were observed between controls and AW_{Hi} subjects in the right caudate ($p = .093$) and between controls and AW_{Lo} in the right GP ($p = .077$; Table 2). The differences between the AW_{Hi} and AW_{Lo} groups were not statistically significant ($p \geq .24$).

Striatal Dopaminergic Transporter (DAT Binding, [123I]-Ioflupane SPECT) Measures

There were no significant hemispheric differences in any striatal DAT binding measures in controls, AW, or the AW subgroups ($p \geq .36$). Comparison of DAT-binding intensity among controls and AW subgroups (high- and low-exposure) also demonstrated no significant difference in striatal subregions ($p \geq .21$; Table 3).

The Relationship of MRI DTI and Dopaminergic Transporter (DAT Binding) Measurements With Exposure Metrics

DTI measures (FA or MD) from the SN, Put, caudate, or GP did not correlate with days of exposure in the overall AW group ($p \geq .17$). DAT-binding measurements also did not correlate with days of exposure ($p \geq .32$; Supplementary Figure 2).

Since SN and GP FA measurements were significantly different between controls and AW, we graphed the relationships between FA measures and days of exposure using the raw data, and presented them in Supplementary Figure 1 for nigral FA and Supplementary Figure 2 for GP FA values.

The Relationship Between DTI and Striatal Dopaminergic Transporter Density

Since SN and GP DTI measures were significantly different between controls and AW, we explored their relationship to striatal DAT-binding measurements. Within controls, there were no significant correlations between any DTI measure and striatal dopaminergic transporter measurements (data not shown). Within AW, right SN FA values negatively correlated with DAT binding in the right posterior striatum ($\rho = -0.489$; $p = .034$; Table 4). In addition, FA values in the left GP correlated

Table 2. DTI Measures in Control and AWs

BG regions	Hemi-sphere	Controls (Con)	AWs			Group comparisons			
			AW	AW_{Lo}	AW_{Hi}	Con vs. AW	Con vs. AW_{Lo}	Con vs. AW_{Hi}	AW_{Hi} vs. AW_{Lo}
FA measures									
SN	Left	0.503 ± 0.043	0.447 ± 0.071	0.463 ± 0.093	0.432 ± 0.040	**0.026***	0.151	**0.017***	0.310
	Right	0.464 ± 0.059	0.445 ± 0.071	0.440 ± 0.073	0.450 ± 0.074	0.476	0.443	0.662	0.746
Caudate	Left	0.223 ± 0.018	0.222 ± 0.027	0.225 ± 0.032	0.219 ± 0.023	0.863	0.934	0.709	0.658
	Right	0.222 ± 0.039	0.218 ± 0.031	0.216 ± 0.038	0.219 ± 0.024	0.726	0.847	0.691	0.842
Put	Left	0.322 ± 0.029	0.310 ± 0.030	0.315 ± 0.034	0.304 ± 0.026	0.280	0.577	0.202	0.477
	Right	0.307 ± 0.027	0.294 ± 0.037	0.296 ± 0.036	0.291 ± 0.040	0.320	0.517	0.303	0.706
GP	Left	0.401 ± 0.030	0.366 ± 0.044	0.371 ± 0.051	0.362 ± 0.038	**0.029***	0.101	**0.037***	0.635
	Right	0.364 ± 0.049	0.337 ± 0.042	0.330 ± 0.046	0.344 ± 0.039	0.126	0.118	0.299	0.592
MD measures									
SN	Left	$8.19 \pm 1.48 \times 10^{-4}$	$8.55 \pm 1.21 \times 10^{-4}$	$8.33 \pm 1.26 \times 10^{-4}$	$8.77 \pm 1.18 \times 10^{-4}$	0.439	0.710	0.350	0.581
	Right	$8.98 \pm 1.96 \times 10^{-4}$	$9.05 \pm 1.25 \times 10^{-4}$	$9.41 \pm 1.29 \times 10^{-4}$	$8.69 \pm 1.16 \times 10^{-4}$	0.886	0.459	0.623	0.236
Caudate	Left	1.049 ± 0.115	1.041 ± 0.212	1.092 ± 0.259	0.990 ± 0.149	0.906	0.630	0.496	0.262
	Right	1.110 ± 0.183	1.040 ± 0.127	1.083 ±0.145	0.998 ± 0.094	0.187	0.562	0.093	0.273
Put	Left	0.744 ± 0.020	0.751 ± 0.030	0.749 ± 0.026	0.752 ± 0.035	0.518	0.756	0.435	0.647
	Right	0.788 ± 0.027	0.794 ± 0.043	0.799 ± 0.028	0.789 ± 0.056	0.638	0.593	0.795	0.788
GP	Left	0.751 ± 0.035	0.789 ± 0.071	0.796 ± 0.091	0.783 ± 0.049	0.109	0.117	0.248	0.671
	Right	0.815 ± 0.040	0.857 ± 0.078	0.872 ± 0.089	0.843 ± 0.068	0.106	0.077	0.319	0.430

Data represent the mean ± SD. DTI measures were compared using ANCOVA with adjustment for age. *p* values are presented for the comparisons among controls, AW, and AW subgroups (Hi and Lo). Asterisks and bolded text represent significant comparisons.

Table 3. Dopamine Transporter Uptake Measures in Controls and AW

	Controls	AWs			Group Comparisons (*p* values)			
		AW	AW_{Lo}	AW_{Hi}	Controls vs. AW	Controls vs. AW_{Lo}	Controls vs. AW_{Hi}	AW_{Hi}vs. AW_{Lo}
Anterior Striatum								
Left	2.51 ± 0.51	2.40 ± 0.34	2.45 ± 0.34	2.34 ± 0.36	0.458	0.807	0.312	0.453
Right	2.44 ± 0.42	2.34 ± 0.32	2.40 ± 0.36	2.27 ± 0.27	0.445	0.953	0.213	0.248
Posterior Striatum								
Left	3.13 ± 0.62	3.17 ± 0.57	3.18 ± 0.68	3.16 ± 0.48	0.817	0.721	0.974	0.752
Right	3.11 ± 0.45	3.19 ± 0.53	3.19 ± 0.60	3.18 ± 0.49	0.650	0.612	0.796	0.807

Data represent the mean ± SD. DAT binding is expressed as a ratio of striatal/occipital cortex binding, and were compared using ANCOVA with adjustment for age. *p* values are presented for the comparisons among controls, AW, AW subgroups (Hi and Lo).

Table 4. Relationships Between DTI FA and DAT Binding Values in AW

	DAT Binding[a]			
	Anterior		Posterior	
	Left	Right	Left	Right
Substantia nigra				
FA				
Left	−0.031	0.090	0.063	−0.177
	0.900	0.717	0.792	0.469
Right	−0.174	0.119	−0.265	**−0.489***
	0.476	0.627	0.273	**0.034**
Globus Pallidus				
FA				
Left	0.256	0.302	**0.459***	0.147
	0.290	0.208	**0.048**	0.548
Right	0.159	0.315	−0.283	0.046
	0.517	0.190	0.241	0.853

[a]Data represent the correlation coefficients (ρ, top number) and the p values (bottom number) of the Spearman partial correlation analyses with adjustment for age. Significant correlations are indicated by bolded text and asterisks.

positively with DAT binding in the left posterior striatal region ($\rho = 0.459$, $p = .048$).

DISCUSSION

The results from this study are consistent with prior cross-sectional findings of SN microstructural changes in AW (Du *et al.*, 2014), but also revealed lower GP values in AW and lateralized (left) vulnerability of these BG structures to pesticide exposure. Conversely, our study did not reveal any DTI differences in striatal structures (caudate and Put). In addition, DAT binding was not decreased in AW as we hypothesized, suggesting that striatal regions are relatively resilient to pesticide neurotoxicity. The finding that nigral and pallidal FA measures are lower only in AW with high, but not low, exposures to pesticide hints at a potential exposure-MRI correlation. The direct correlation analysis, however, did not detect a significant association, which could be due to the small sample size. Collectively, these results suggest a lateralized and selective BG signature that can be captured by DTI may reflect damage due to occupational pesticide exposure among agricultural workers.

SN and GP Microstructural Changes as Markers of Pesticide Related Neurotoxicity

Lower SN FA values in AW observed previously (Du *et al.*, 2014) and in the current study were in a similar to, but less severe, than those seen in PD patients (Du *et al.*, 2012; Ofori *et al.*, 2015; Prodoehl *et al.*, 2009). The exact mechanism and implications of this DTI finding are unknown. Given the evidence from animal (Boska *et al.*, 2007) and epidemiological (McCormack *et al.*, 2002; Pezzoli and Cereda, 2013; Tanner *et al.*, 2011) studies, one may hypothesize that this microstructural signature may reflect dopaminergic cell loss similar to that in PD. Yet no striatal field difference in DAT-binding argues against this hypothesis. There is a view that that PD may be caused by multiple "hits" (Hawkes *et al.*, 2007; Sulzer, 2007), and the microstructural findings detected by DTI may mark one of these vulnerabilities. These nigral findings do not represent PD pathology *per se*, but rather a proximal event that may make exposed individuals more susceptible to a "next" hit that will cumulatively lead to PD.

We also discovered decreased GP FA values in AW, especially those with higher exposure levels. These data suggest that the GP, like the nigra, is vulnerable to pesticide exposure. The GP has higher energy demands, is a "sink" for divalent ions (eg, iron, manganese, copper, etc.), and displays FA alterations even at relatively low exposure levels (Lee *et al.*, 2015). Yet GP FA alterations have not been described in PD patients or in our own dataset (unpublished). It is increasingly recognized, however, that REM behavior disorder is associated with the development of neurodegenerative disease, particularly α-synucleinopathies (eg, PD, multisystem atrophy, and Lewy body dementia; Boeve, 2010; Iranzo *et al.*, 2006, 2013; Schenck *et al.*, 1996). Radiotracer imaging in this prodromal population indicates increased metabolism in the GP (Holtbernd *et al.*, 2014). Thus, it will be very interesting in the future to see if the GP FA differences observed in the current study may be related to GP metabolism. Our exploratory correlation analyses showed that lower left GP FA values may be associated with lower left Put (posterior striatal) DAT binding (Table 4). The traditional view suggests that the nigra projects to the striatum that then connects to the GP internus through the direct or indirect pathway (DeLong *et al.*, 1984). Several recent studies, however, have reported that the GP, particularly the GP externus (GPe), projects to the dorsal striatum (reviewed by Hegeman *et al.*, 2016). A systematic analysis of GPe inputs to the dorsal striatum currently is lacking, but it is possible that microstructural changes in the GP (reflected by lower FA values) could precipitate nigrostriatal dopaminergic terminal alterations that ultimately lead to PD vulnerability. Further studies are warranted to investigate both nigral and pallidal DTI modifications as biomarkers for pesticide-related toxicity.

Lateralized SN Change and Its Significance to the Asymmetrical Onset of PD Symptoms

The finding of lateralized vulnerability of the left SN and GP in AW is consistent with previous studies in PD indicating that the dominant hemisphere is more vulnerable to insult (Filippi *et al.*, 1995). Previous studies also have suggested that handedness and hemisphere dominance may play a role in the development of PD symptoms (Barrett *et al.*, 2011; Haaxma *et al.*, 2010; Scherfler *et al.*, 2012). Indeed, Uitti *et al.* (2005) demonstrated that right handed PD patients have a greater likelihood of having right- rather than left-side symptoms, although handedness explained relatively little of the variance (approximately 20%) associated with asymmetric onset in PD. Lower left SN FA values have been reported previously in PD patients (Prakash *et al.*, 2012). Furthermore, Scherfler *et al.* (2012) measured dopamine transporter labeling in right-handed PD subjects and found a preponderance of lower left putaminal binding, asserting that the vulnerability of SN neurons may not be random. To our knowledge, this study is the first demonstration of lateralized vulnerability of the BG to environmental toxins.

The exact cause of the lateralized vulnerability, however, is unclear. In this study, left BG DTI measures were higher than right side values in control subjects. Whereas the higher SN FA values may symbolize better organization and efficiency of this hemisphere, it also may represent higher energy demands and its vulnerability to neurotoxins. Future studies regarding the timing of lateralized BG FA differences in the brain may be extremely useful in understanding neurodevelopment and may shed light on its contribution to the asymmetric onset of PD.

Relative Resilience of Striatal Dopaminergic Transporters and the Possibility of Contralateral Compensation

In our study, nigral and GP microstructural changes in AW occurred in the absence of DTI or DAT binding differences in any striatal region. These data suggest that striatal

dopaminergic terminals are more resilient to pesticide exposure and microstructural alterations in the SN/GP occur prior to or without evidence of dopamine transporter loss. These results are contrary to our original hypothesis. An alternative hypothesis is that there are compensatory increases in dopamine transporters that occur in response to perturbation (Castro-Hernandez *et al.*, 2015; Gordon *et al.*, 1996; Kimmel *et al.*, 2001; Lee *et al.*, 2000; Meiergerd *et al.*, 1993) as has been shown in animal models (Mamaligas *et al.*, 2016) and humans (Berry *et al.*, 2016; Rossi *et al.*, 2017).

Interestingly, we observed significant associations between nigral DTI and DAT-binding measurements. Namely, right nigral FA measures correlated negatively with DAT binding in the right posterior striatum, the region known to be affected early in PD patients (Fearnley and Lees, 1991). Although nigral projections are primarily to the ipsilateral striatum, several studies have demonstrated contralateral projections in rodent models (Douglas *et al.*, 1987; Veening *et al.*, 1980), suggesting that approximately 3% of nigral projections are contralateral. Additional studies have shown electrophysiological and neurochemical changes in the striatum that result from manipulations of the contralateral nigra (Castellano and Rodriguez Diaz, 1991; Lawler *et al.*, 1995; Nieoullon *et al.*, 1979). Thus, it is possible that the compromise in the left SN may preferentially affect the left striatum such that it sends a "help" signal to the right nigrostriatal pathway that then assumes a predominant compensatory role for deficits in the left circuit. Consistent with this hypothesis, previous studies have suggested compensatory brain mechanisms may occur both in animal models exposed to a perturbation (Blanchard *et al.*, 1996; Dravid *et al.*, 1984) and in patients with neurological disorders (Lewis *et al.*, 2011; Mufson *et al.*, 2015).

Limitations of Our Studies and Future Directions

Despite the intriguing nature of the results, our study has several limitations. First, although the number of subjects is similar to that in many imaging studies, the sample size is relatively small. Second, previous research has indicated that FA values are affected by age and factors such as diet and socio-economic status (Salat *et al.*, 2005; Vaillancourt *et al.*, 2012; Wu *et al.*, 2011). In our statistical analyses, we accounted for age, but not diet and socio-economic status. Third, there was a wide range of exposures in our AW cohort, with only a sparse sample with >1000 days of exposure that limited our attempt to correlate the exposure measurement with our imaging findings. We tried to mitigate this by separating the AWs into 2 groups based on the median days of exposure, but additional subjects are needed to fill in the sparse areas. Fourth, AWs are exposed to multiple pesticides, and there is no known biomarker (blood, urine, etc) to reflect past pesticide exposure. Thus, we were unable to determine the exact chemical(s) that may have contributed to the current findings.

Summary

This study demonstrated a lateralized microstructural signature in the BG that may be related to chronic pesticide exposure, with the left SN and GP being more vulnerable than the right, and striatal structures being more resistant. These occur without deficits in dopamine transporter density that is marked in PD. Our study also hinted that right nigrostriatal circuitry may compensate when pesticides insult the left pathway. These findings need to be replicated in larger cohorts and with longitudinal designs because they may be extremely important in understanding pesticide-related neurotoxicity and its link to PD-related pathoetiology.

SUPPLEMENTARY DATA

Supplementary data are available at *Toxicological Sciences* online.

ACKNOWLEDGMENTS

We express gratitude to all of the participants who volunteered for this study and the study personnel who contributed to its completion. We also thank Mr John Bray and Ms Melissa Santos for their efforts in recruiting study participants and coordinating the study.

FUNDING

This work was supported in part by the National Institute of Neurological Disease and Stroke (NS060722 and NS082151 to X.H.), the National Institute of Environmental Health Sciences (ES022614 to B.C.J.), the Hershey Medical Center General Clinical Research Center (National Center for Research Resources, Grant UL1 RR033184 that is now at the National Center for Advancing Translational Sciences, Grant UL1 TR000127), and a GE HealthCare grant. All analyses, interpretations, and conclusions are those of the authors and not the research sponsors.

REFERENCES

Avants, B. B., Tustison, N. J., Song, G., Cook, P. A., Klein, A., and Gee, J. C. (2011). A reproducible evaluation of ANTs similarity metric performance in brain image registration. *Neuroimage* **54**, 2033–2044.

Barrett, M. J., Wylie, S. A., Harrison, M. B., and Wooten, G. F. (2011). Handedness and motor symptom asymmetry in Parkinson's disease. *J. Neurol. Neurosurg. Psychiatry.* **82**, 1122–1124.

Berry, A. S., Shah, V. D., Baker, S. L., Vogel, J. W., O'Neil, J. P., Janabi, M., Schwimmer, H. D., Marks, S. M., and Jagust, W. J. (2016). Aging affects dopaminergic neural mechanisms of cognitive flexibility. *J. Neurosci.* **36**, 12559–12569.

Blanchard, V., Anglade, P., Dziewczapolski, G., Savasta, M., Agid, Y., and Raisman-Vozari, R. (1996). Dopaminergic sprouting in the rat striatum after partial lesion of the substantia nigra. *Brain Res.* **709**, 319–325.

Boeve, B. F. (2010). REM sleep behavior disorder: Updated review of the core features, the REM sleep behavior disorder-neurodegenerative disease association, evolving concepts, controversies, and future directions. *Ann. N. Y. Acad. Sci.* **1184**, 15–54.

Boska, M. D., Hasan, K. M., Kibuule, D., Banerjee, R., McIntyre, E., Nelson, J. A., Hahn, T., Gendelman, H. E., and Mosley, R. L. (2007). Quantitative diffusion tensor imaging detects dopaminergic neuronal degeneration in a murine model of Parkinson's disease. *Neurobiol. Dis.* **26**, 590–596.

Castellano, M. A., and Rodriguez Diaz, M. (1991). Nigrostriatal dopaminergic cell activity is under control by substantia nigra of the contralateral brain side: Electrophysiological evidence. *Brain Res. Bull.* **27**, 213–218.

Castro-Hernandez, J., Afonso-Oramas, D., Cruz-Muros, I., Salas-Hernandez, J., Barroso-Chinea, P., Moratalla, R., Millan, M. J., and Gonzalez-Hernandez, T. (2015). Prolonged treatment with pramipexole promotes physical interaction of striatal dopamine D3 autoreceptors with dopamine transporters to reduce dopamine uptake. *Neurobiol. Dis.* **74**, 325–335.

Chan, L. L., Rumpel, H., Yap, K., Lee, E., Loo, H. V., Ho, G. L., Fook-Chong, S., Yuen, Y., and Tan, E. K. (2007). Case control study of diffusion tensor imaging in Parkinson's disease. *J. Neurol. Neurosurg. Psychiatry*. **78**, 1383–1386.

DeLong, M. R., Alexander, G. E., Georgopoulos, A. P., Crutcher, M. D., Mitchell, S. J., and Richardson, R. T. (1984). Role of basal ganglia in limb movements. *Hum. Neurobiol.* **2**, 235–244.

Desplats, P., Patel, P., Kosberg, K., Mante, M., Patrick, C., Rockenstein, E., Fujita, M., Hashimoto, M., and Masliah, E. (2012). Combined exposure to Maneb and Paraquat alters transcriptional regulation of neurogenesis-related genes in mice models of Parkinson's disease. *Mol. Neurodegener.* **7**, 49.

Dickson, D. W., Braak, H., Duda, J. E., Duyckaerts, C., Gasser, T., Halliday, G. M., Hardy, J., Leverenz, J. B., Del, T. K., Wszolek, Z. K., *et al.* (2009). Neuropathological assessment of Parkinson's disease: Refining the diagnostic criteria. *Lancet Neurol.* **8**, 1150–1157.

Douglas, R., Kellaway, L., Mintz, M., and van Wageningen, G. (1987). The crossed nigrostriatal projection decussates in the ventral tegmental decussation. *Brain Res.* **418**, 111–121.

Dravid, A., Jaton, A. L., Enz, A., and Frei, P. (1984). Spontaneous recovery from motor asymmetry in adult rats with 6-hydroxydopamine-induced partial lesions of the substantia nigra. *Brain Res.* **311**, 361–365.

Du, G., Lewis, M. M., Sen, S., Wang, J., Shaffer, M. L., Styner, M., Yang, Q. X., and Huang, X. (2012). Imaging nigral pathology and clinical progression in Parkinson's disease. *Mov. Disord.* **27**, 1636–1643.

Du, G., Lewis, M. M., Sterling, N. W., Kong, L., Chen, H., Mailman, R. B., and Huang, X. (2014). Microstructural changes in the substantia nigra of asymptomatic agricultural workers. *Neurotoxicol. Teratol.* **41**, 60–64.

Du, G., Lewis, M. M., Styner, M., Shaffer, M. L., Sen, S., Yang, Q. X., and Huang, X. (2011). Combined R2* and diffusion tensor imaging changes in the substantia nigra in Parkinson's disease. *Mov. Disord.* **26**, 1627–1632.

Fearnley, J. M., and Lees, A. J. (1991). Ageing and Parkinson's disease: Substantia nigra regional selectivity. *Brain.* **114**, 2283–2301.

Filippi, M., Martino, G., Mammi, S., Campi, A., Comi, G., and Grimaldi, L. M. (1995). Does hemispheric dominance influence brain lesion distribution in multiple sclerosis? *J Neurol. Neurosurg. Psychiatry* **58**, 748–749.

Gordon, I., Weizman, R., and Rehavi, M. (1996). Modulatory effect of agents active in the presynaptic dopaminergic system on the striatal dopamine transporter. *Eur. J. Pharmacol.* **298**, 27–30.

Gouttard, S., Styner, M., Joshi, S., Smith, R. G., Hazlett, H. C., and Gerig, G. (2007) Subcortical structure segmentation using probabilistic atlas priors. Medical Imaging. International Society for Optics and Photonics, pp. 65111-651221.

Haaxma, C. A., Helmich, R. C., Borm, G. F., Kappelle, A. C., Horstink, M. W., and Bloem, B. R. (2010). Side of symptom onset affects motor dysfunction in Parkinson's disease. *Neuroscience* **170**, 1282–1285.

Hawkes, C. H., Del, T. K., and Braak, H. (2007). Parkinson's disease: A dual-hit hypothesis. *Neuropathol. Appl. Neurobiol.* **33**, 599–614.

Hegeman, D. J., Hong, E. S., Hernandez, V. M., and Chan, C. S. (2016). The external globus pallidus: Progress and perspectives. *Eur. J. Neurosci.* **43**, 1239–1265.

Holtbernd, F., Gagnon, J. F., Postuma, R. B., Ma, Y., Tang, C. C., Feigin, A., Dhawan, V., Vendette, M., Soucy, J. P., Eidelberg, D., *et al.* (2014). Abnormal metabolic network activity in REM sleep behavior disorder. *Neurology* **82**, 620–627.

Iranzo, A., Molinuevo, J. L., Santamaria, J., Serradell, M., Marti, M. J., Valldeoriola, F., and Tolosa, E. (2006). Rapid-eye-movement sleep behaviour disorder as an early marker for a neurodegenerative disorder: A descriptive study. *Lancet Neurol.* **5**, 572–577.

Iranzo, A., Tolosa, E., Gelpi, E., Molinuevo, J. L., Valldeoriola, F., Serradell, M., Sanchez-Valle, R., Vilaseca, I., Lomena, F., Vilas, D., *et al.* (2013). Neurodegenerative disease status and post-mortem pathology in idiopathic rapid-eye-movement sleep behaviour disorder: An observational cohort study. *Lancet Neurol.* **12**, 443–453.

Kimmel, H. L., Joyce, A. R., Carroll, F. I., and Kuhar, M. J. (2001). Dopamine D1 and D2 receptors influence dopamine transporter synthesis and degradation in the rat. *J Pharmacol. Exp. Ther.* **298**, 129–140.

Kupsch, A. R., Bajaj, N., Weiland, F., Tartaglione, A., Klutmann, S., Buitendyk, M., Sherwin, P., Tate, A., and Grachev, I. D. (2012). Impact of DaTscan SPECT imaging on clinical management, diagnosis, confidence of diagnosis, quality of life, health resource use and safety in patients with clinically uncertain parkinsonian syndromes: A prospective 1-year follow-up of an open-label controlled study. *J. Neurol. Neurosurg. Psychiatry* **83**, 620–628.

Lawler, C. P., Gilmore, J. H., Watts, V. J., Walker, Q. D., Southerland, S. B., Cook, L. L., Mathis, C. A., and Mailman, R. B. (1995). Interhemispheric modulation of dopamine receptor interactions in unilateral 6-OHDA rodent model. *Synapse* **21**, 299–311.

Le Bihan, D., Mangin, J. F., Poupon, C., Clark, C. A., Pappata, S., Molko, N., and Chabriat, H. (2001). Diffusion tensor imaging: Concepts and applications. *J. Magn. Reson. Imaging* **13**, 534–546.

Lee, C. S., Samii, A., Sossi, V., Ruth, T. J., Schulzer, M., Holden, J. E., Wudel, J., Pal, P. K., de, lF-F., Calne, D. B., *et al.* (2000). In vivo positron emission tomographic evidence for compensatory changes in presynaptic dopaminergic nerve terminals in Parkinson's disease. *Ann. Neurol.* **47**, 493–503.

Lee, E. Y., Flynn, M. R., Du, G., Lewis, M. M., Fry, R., Herring, A. H., Van Buren, E., Van Buren, S., Smeester, L., Kong, L., *et al.* (2015). T1 relaxation rate (R1) indicates nonlinear Mn accumulation in brain tissue of welders with low-level exposure. *Toxicol. Sci.* **146**, 281–289.

Lee, E. Y., Flynn, M. R., Du, G., Lewis, M. M., Herring, A. H., Van Buren, E., Van Buren, S., Kong, L., Mailman, R. B., and Huang, X. (2016). Highlight: Lower fractional anisotropy in the globus pallidus of asymptomatic welders, a marker for long-term welding exposure. *Toxicol. Sci.* **153**, 165–173.

Lewis, M. M., Du, G., Sen, S., Kawaguchi, A., Truong, Y., Lee, S., Mailman, R. B., and Huang, X. (2011). Differential involvement of striato- and cerebello-thalamo-cortical pathways in tremor- and akinetic/rigid-predominant Parkinson's disease. *Neuroscience* **177**, 230–239.

Liu, Z., Wang, Y., Gerig, G., Gouttard, S., Tao, R., Fletcher, T., and Styner, M. (2010) Quality control of diffusion weighted images. Proceedings of SPIE–the International Society for Optical Engineering, Mar 11, 7628.

Mamaligas, A. A., Cai, Y., and Ford, C. P. (2016). Nicotinic and opioid receptor regulation of striatal dopamine D2-receptor mediated transmission. *Sci Rep* **6**, 37834.

Martin, W. R., Wieler, M., and Gee, M. (2008). Midbrain iron content in early Parkinson disease: A potential biomarker of disease status. *Neurology* **70**, 1411–1417.

Massey, L. A., and Yousry, T. A. (2010). Anatomy of the substantia nigra and subthalamic nucleus on MR imaging. *Neuroimaging Clin. N. Am.* **20**, 7–27.

McCormack, A. L., Thiruchelvam, M., Manning-Bog, A. B., Thiffault, C., Langston, J. W., Cory-Slechta, D. A., and Di Monte, D. A. (2002). Environmental risk factors and Parkinson's disease: Selective degeneration of nigral dopaminergic neurons caused by the herbicide paraquat. *Neurobiol. Dis.* **10**, 119–127.

Meiergerd, S. M., Patterson, T. A., and Schenk, J. O. (1993). D2 receptors may modulate the function of the striatal transporter for dopamine: Kinetic evidence from studies in vitro and in vivo. *J. Neurochem.* **61**, 764–767.

Mufson, E. J., Mahady, L., Waters, D., Counts, S. E., Perez, S. E., DeKosky, S. T., Ginsberg, S. D., Ikonomovic, M. D., Scheff, S. W., and Binder, L. I. (2015). Hippocampal plasticity during the progression of Alzheimer's disease. *Neuroscience* **309**, 51–67.

Nieoullon, A., Cheramy, A., Leviel, V., and Glowinski, J. (1979). Effects of the unilateral nigral application of dopaminergic drugs on the in vivo release of dopamine in the two caudate nuclei of the cat. *Eur. J. Pharmacol.* **53**, 289–296.

Ofori, E., Pasternak, O., Planetta, P. J., Li, H., Burciu, R. G., Snyder, A. F., Lai, S., Okun, M. S., and Vaillancourt, D. E. (2015) Longitudinal changes in free-water within the substantia nigra of Parkinson's disease. *Brain* **138** (Pt8), 2322–2331.

Peran, P., Cherubini, A., Assogna, F., Piras, F., Quattrocchi, C., Peppe, A., Celsis, P., Rascol, O., Demonet, J. F., Stefani, A., *et al.* (2010). Magnetic resonance imaging markers of Parkinson's disease nigrostriatal signature. *Brain* **133**, 3423–3433.

Pezzoli, G., and Cereda, E. (2013). Exposure to pesticides or solvents and risk of Parkinson disease. *Neurology* **80**, 2035–2041.

Prakash, B. D., Sitoh, Y. Y., Tan, L. C., and Au, W. L. (2012). Asymmetrical diffusion tensor imaging indices of the rostral substantia nigra in Parkinson's disease. *Parkinsonism Relat. Disord.* **18**, 1029–1033.

Prodoehl, J., Corcos, D. M., and Vaillancourt, D. E. (2009). Basal ganglia mechanisms underlying precision grip force control. *Neurosci. Biobehav. Rev.* **33**, 900–908.

Riederer, P., and Sian-Hulsmann, J. (2012). The significance of neuronal lateralisation in Parkinson's disease. *J. Neural Transm.* **119**, 953–962.

Rossi, C., Genovesi, D., Marzullo, P., Giorgetti, A., Filidei, E., Corsini, G. U., Bonuccelli, U., and Ceravolo, R. (2017). Striatal dopamine transporter modulation after rotigotine: Results from a pilot single-photon emission computed tomography study in a group of early stage parkinson disease patients. *Clin. Neuropharmacol.* **40**(1), 34–36.

Rueckert, D., Sonoda, L. I., Hayes, C., Hill, D. L., Leach, M. O., and Hawkes, D. J. (1999). Nonrigid registration using free-form deformations: Application to breast MR images. *Med. Imag. IEEE Trans.* **18**, 712–721.

Salat, D. H., Tuch, D. S., Greve, D. N., van der Kouwe, A. J., Hevelone, N. D., Zaleta, A. K., Rosen, B. R., Fischl, B., Corkin, S., Rosas, H. D., *et al.* (2005). Age-related alterations in white matter microstructure measured by diffusion tensor imaging. *Neurobiol. Aging* **26**, 1215–1227.

Salvador, R., Pena, A., Menon, D. K., Carpenter, T. A., Pickard, J. D., and Bullmore, E. T. (2005). Formal characterization and extension of the linearized diffusion tensor model. *Hum. Brain Mapp.* **24**, 144–155.

Schenck, C. H., Bundlie, S. R., and Mahowald, M. W. (1996). Delayed emergence of a parkinsonian disorder in 38% of 29 older men initially diagnosed with idiopathic rapid eye movement sleep behaviour disorder. *Neurology* **46**, 388–393.

Scherfler, C., Seppi, K., Mair, K. J., Donnemiller, E., Virgolini, I., Wenning, G. K., and Poewe, W. (2012). Left hemispheric predominance of nigrostriatal dysfunction in Parkinson's disease. *Brain* **135**, 3348–3354.

Seibyl, J. P., Marek, K. L., Quinlan, D., Sheff, K., Zoghbi, S., Zea-Ponce, Y., Baldwin, R. M., Fussell, B., Smith, E. O., and Charney, D. S. (1995). Decreased single-photon emission computed tomographic [123I]beta-CIT striatal uptake correlates with symptom severity in Parkinson's disease. *Ann. Neurol.* **38**, 589–598.

Sulzer, D. (2007). Multiple hit hypotheses for dopamine neuron loss in Parkinson's disease. *Trends Neurosci.* **30**, 244–250.

Tanner, C. M., Kamel, F., Ross, G. W., Hoppin, J. A., Goldman, S. M., Korell, M., Marras, C., Bhudhikanok, G. S., Kasten, M., Chade, A. R., *et al.* (2011). Rotenone, paraquat, and Parkinson's disease. *Environ. Health Perspect.* **119**, 866–872.

Tanner, C. M., Ottman, R., Goldman, S. M., Ellenberg, J., Chan, P., Mayeux, R., and Langston, J. W. (1999). Parkinson disease in twins: An etiologic study. *Jama* **281**, 341–346.

Uitti, R. J., Baba, Y., Whaley, N. R., Wszolek, Z. K., and Putzke, J. D. (2005). Parkinson disease: Handedness predicts asymmetry. *Neurology* **64**, 1925–1930.

Uversky, V. N. (2004). Neurotoxicant-induced animal models of Parkinson's disease: Understanding the role of rotenone, maneb and paraquat in neurodegeneration. *Cell Tissue Res.* **318**, 225–241.

Vaillancourt, D. E., Spraker, M. B., Prodoehl, J., Abraham, I., Corcos, D. M., Zhou, X. J., Comella, C. L., and Little, D. M. (2009). High-resolution diffusion tensor imaging in the substantia nigra of de novo Parkinson disease. *Neurology* **72**, 1378–1384.

Vaillancourt, D. E., Spraker, M. B., Prodoehl, J., Zhou, X. J., and Little, D. M. (2012). Effects of aging on the ventral and dorsal substantia nigra using diffusion tensor imaging. *Neurobiol. Aging* **33**, 35–42.

Veening, J. G., Cornelissen, F. M., and Lieven, P. A. (1980). The topical organization of the afferents to the caudatoputamen of the rat. A horseradish peroxidase study. *Neuroscience* **5**, 1253–1268.

Wirdefeldt, K., Gatz, M., Schalling, M., and Pedersen, N. L. (2004). No evidence for heritability of Parkinson disease in Swedish twins. *Neurology* **63**, 305–311.

Wu, T., Wang, L., Hallett, M., Chen, Y., Li, K., and Chan, P. (2011). Effective connectivity of brain networks during self-initiated movement in Parkinson's disease. *Neuroimage* **55**, 204–215.

Yushkevich, P. A., Piven, J., Hazlett, H. C., Smith, R. G., Ho, S., Gee, J. C., and Gerig, G. (2006). User-guided 3D active contour segmentation of anatomical structures: Significantly improved efficiency and reliability. *Neuroimage* **31**, 1116–1128.